Self-Balancing of the Clamping-Capacitor-Voltages in the Multilevel Capacitor-Clamping-Inverter under Sub-Harmonic PWM Modulation

Xiaoming Yuan, *Member, IEEE*, Herbert Stemmler, and Ivo Barbi, *Senior Member, IEEE*

***Abstract*—The paper explores the spontaneous coupled clamping-capacitor-current control loops and the resultant self-balancing property of the clamping-capacitor-voltages in the multilevel capacitor-clamping-inverter. The case of the three-level capacitor-clamping-inverter under sub-harmonic PWM modulation is dealt with first. The case of the multilevel capacitor-clamping-inverter ($M > 3$) under sub-harmonic PWM modulation is then analyzed. Test results on a half-bridge three-level capacitor-clamping-inverter prototype under sub-harmonic PWM modulation are demonstrated in the end.**

***Index Terms*—Capacitor-clamping-inverter, clamping-capacitor-voltage, self-balancing, sub-harmonic PWM modulation.**

I. Introduction

MULTILEVEL inverters [1], [2] have been attracting wide industrial interests recently. Among the major topologies, the multilevel diode-clamping-inverter suffers from problems such as dc link voltage unbalance [3], [4], excessive number of clamping diodes, indirect clamping of the inner switches and diodes etc. [5]. Further, as at any moment only one switching cell in an inverter leg is allowed to operate, the inverter leg output frequency is actually limited to the instantaneous frequency of the switching cells, instead of being multiplied. The multilevel cascading inverter, despite the constraint of isolated dc sides, has been successfully commercialized for medium voltage drive [6] and reactive power compensating [7] applications, new developments are also under way [8]–[10]. The multilevel capacitor-clamping-inverter, with the rating limited to the heat capacity of the clamping capacitors, has also been practically used [11], [12], and seems yet to be another promising alternative.

One of the most crucial concerns over the multilevel capacitor-clamping-inverter is the stability of the clamping-capacitor-voltages. The self-balancing phenomenon of the clamping-capacitor-voltages was physically interpreted in [13]. It is the objective of this paper to report a novel insight into the mechanism of the self-balancing phenomenon in the multilevel capacitor-clamping-inverter.

Manuscript received January 14, 2000; revised December 4, 2000. Recommended by Associate Editor F. Z. Peng.

X. Yuan and H. Stemmler are with the Power Electronics and Electrometrology Laboratory, Swiss Federal Institute of Technology Zurich, Zurich CH-8092, Switzerland (e-mail: yuan@lem.ee.ethz.ch).

I. Barbi is with the Power Electronics Institute, Federal University of Santa Catarina, Florianopolis-SC 88040-970, Brazil (e-mail: ivo.barbi@inep.ufsc.br).

Publisher Item Identifier S 0885-8993(01)02192-5.

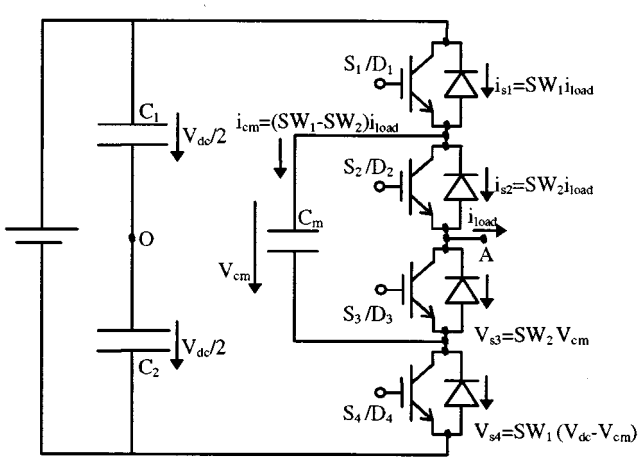

Fig. 1. Structure of a half-bridge three-level capacitor-clamping-inverter.

II. Clamping-Capacitor-Voltage Self-Balancing in the Three-Level Capacitor-Clamping-Inverter under Sub-Harmonic PWM Modulation

A. Sub-Harmonic PWM Modulation

As shown in Fig. 1, a three-level capacitor-clamping-inverter leg consists of two switching cells. S_1/D_1 and S_4/D_4 clamped by the dc link together with the clamping capacitor C_m work alternatively forming the first switching cell, while S_2/D_2 and S_3/D_3 clamped by the clamping capacitor C_m work alternatively forming the second switching cell. To maintain steady state stability of the clamping-capacitor-voltage, the instantaneous duty cycles of the two switching cells must be equal to each other. On the other hand, to maintain optimum load voltage spectrum, the control signals for the two switching cells must be phase-shifted by π to each other [13]. Such control signals can be generated by the conventional sub-harmonic PWM modulation [14], as shown in Fig. 2.

Also shown in Fig. 2 are the corresponding clamping-capacitor-current $i_{\rm cm}$ and the load voltage of the half-bridge inverter $V_{\rm AO}$. It is observed that as the clamping-capacitor-voltage $V_{\rm cm}$ deviates from its nominal value $V_{\rm dc}/2$ ($V_{\rm cm} < V_{\rm dc}/2$ for the shown case), a switching frequency component $\Delta V_{\rm AO}$ appears in the load voltage $V_{\rm AO}$.

B. Mechanism of the Spontaneous Clamping-Capacitor-Current Control Loop

Due to charge (amp-s) balance of the clamping capacitor, the inverter is deemed at steady state in terms of the clamping-

capacitor-voltage so long as the dc component of the current flowing through the clamping capacitor is zero. If for any reason this dc component deviates from zero, the clamping capacitor will be charged or discharged leading to load voltage variation, load current variation, and in turn dc component variation in the clamping-capacitor-current. As will be verified in the following, under sub-harmonic PWM modulation, such dc component variation will discharge or charge the clamping capacitor until the dc component in the clamping-capacitor-current returns to zero. This spontaneous clamping-capacitor-current control loop is illustrated in Fig. 3.

C. Verification of the Spontaneous Clamping-Capacitor-Current Control Loop

The switching functions SW_1 and SW_2 generated from the sub-harmonic PWM modulation, as shown in Fig. 2, can be expressed in Fourier form by (1) and (2)

$$\begin{aligned}\mathrm{sw}_1 &= \frac{1}{2} + \frac{M}{2}\sin(\omega_m t) \\ &\quad + \sum_{m=1,3,5\ldots}^{\infty} (-1)^{\frac{m+1}{2}} \frac{2J_0^{\frac{mM\pi}{2}}}{m\pi} \sin\left(m\omega_c t - \frac{\pi}{2}\right) \\ &\quad + \sum_{m=1,3,5\ldots}^{\infty} \sum_{n=\pm 2,\pm 4,\ldots}^{\pm\infty} \frac{2J_n^{\frac{mM\pi}{2}}}{m\pi} \\ &\quad \times \sin\left(\frac{m\pi}{2}\right) \cos[(m\omega_c t + n\omega_m t) - m\pi] \\ &\quad + \sum_{m=2,4,\ldots}^{\infty} \sum_{n=\pm 1,\pm 3,\ldots}^{\pm\infty} \frac{2J_n^{\frac{mM\pi}{2}}}{m\pi} \\ &\quad \times \cos\left(\frac{m\pi}{2}\right) \sin[(m\omega_c t + n\omega_m t) - m\pi] \qquad (1)\end{aligned}$$

$$\begin{aligned}\mathrm{sw}_2 &= \frac{1}{2} + \frac{M}{2}\sin(\omega_m t) \\ &\quad - \sum_{m=1,3,5\ldots}^{\infty} (-1)^{\frac{m+1}{2}} \frac{2J_0^{\frac{mM\pi}{2}}}{m\pi} \sin\left(m\omega_c t - \frac{\pi}{2}\right) \\ &\quad - \sum_{m=1,3,5\ldots}^{\infty} \sum_{n=\pm 2,\pm 4,\ldots}^{\pm\infty} \frac{2J_n^{\frac{mM\pi}{2}}}{m\pi} \\ &\quad \times \sin\left(\frac{m\pi}{2}\right) \cos[(m\omega_c t + n\omega_m t) - m\pi] \\ &\quad + \sum_{m=2,4,\ldots}^{\infty} \sum_{n=\pm 1,\pm 3,\ldots}^{\pm\infty} \frac{2J_n^{\frac{mM\pi}{2}}}{m\pi} \\ &\quad \times \cos\left(\frac{m\pi}{2}\right) \sin[(m\omega_c t + n\omega_m t) - m\pi] \qquad (2)\end{aligned}$$

where $J_n^{((mM\pi)/2)}$ is the Bessel function of the first kind and n-th order of argument $(mM\pi)/2$.

The load voltage of the half-bridge inverter V_{AO} can be given as

$$V_{\mathrm{AO}} = \mathrm{sw}_2 V_{\mathrm{cm}} + \mathrm{sw}_1(V_{\mathrm{dc}} - V_{\mathrm{cm}}) - \frac{V_{\mathrm{dc}}}{2} \qquad (3)$$

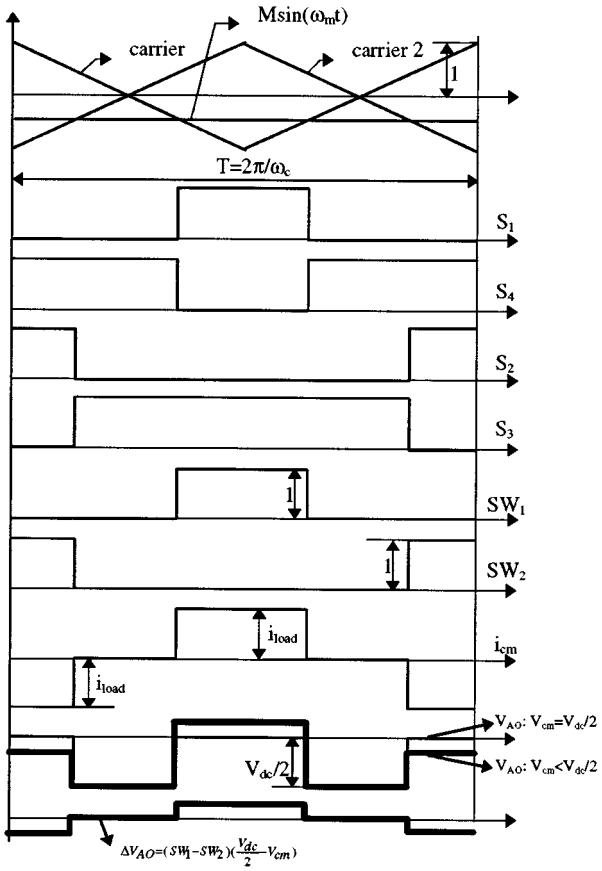

Fig. 2. Sub-harmonic PWM modulation for the half-bridge three-level capacitor-clamping-inverter, with load current in the positive direction. M: modulation index; ω_m: modulating angular frequency; ω_c: carrier angular frequency; T: switching period.

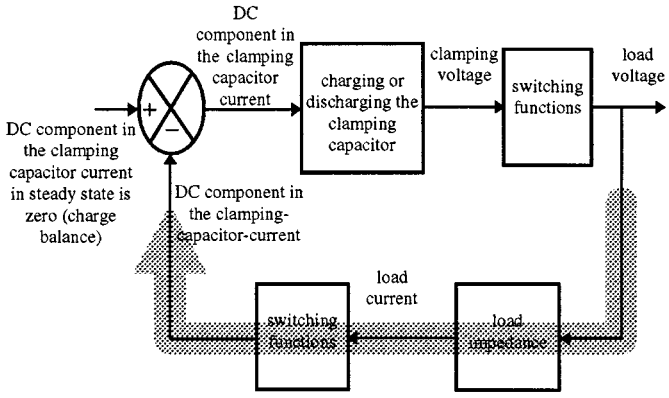

Fig. 3. Spontaneous clamping-capacitor-current control loop in the half-bridge three-level capacitor-clamping-inverter.

which can be rearranged as

$$\begin{aligned}V_{\mathrm{AO}} &= \frac{V_{\mathrm{dc}}}{2}(\mathrm{sw}_1 + \mathrm{sw}_2 - 1) + (\mathrm{sw}_1 - \mathrm{sw}_2) \\ &\quad \times \left(\frac{V_{\mathrm{dc}}}{2} - V_{\mathrm{cm.steady}}\right) \\ &\quad + (\mathrm{sw}_1 - \mathrm{sw}_2)(V_{\mathrm{cm.steady}} - V_{\mathrm{cm}}) \qquad (4)\end{aligned}$$

where $V_{\rm dc}/2$ is the nominal value of the clamping-capacitor-voltage, and $V_{\rm cm.steady}$ is the steady state value of the clamping-capacitor-voltage. In particular, the third part in (4) represents the load voltage variation in response to the deviation of the clamping-capacitor-voltage away from its steady state value.

Substituting from (1) and (2) in the third part of (4), the load voltage variation $\Delta V_{\rm AO}$ can be given by

$$\Delta V_{\rm AO} = (V_{\rm cm.steady} - V_{\rm cm}) \times \left\{ \sum_{m=1,3,5\ldots}^{\infty} (-1)^{\frac{m+1}{2}} \frac{4J_0^{\frac{mM\pi}{2}}}{m\pi} \sin\left(m\omega_c t - \frac{\pi}{2}\right) + \sum_{m=1,3,5\ldots}^{\infty} \sum_{n=\pm 2,\pm 4,\ldots}^{\pm\infty} \frac{4J_n^{\frac{mM\pi}{2}}}{m\pi} \times \sin\left(\frac{m\pi}{2}\right) \cos[(m\omega_c t + n\omega_m t) - m\pi] \right\}. \quad (5)$$

Giving $z_j \angle\theta_j$ representing the load impedance at the harmonic frequency of j, the load current variation $\Delta i_{\rm load}$ resulting from the load voltage variation can be written as (6)

$$\Delta i_{\rm load} = (V_{\rm cm.steady} - V_{\rm cm}) \left\{ \sum_{m=1,3,5\ldots}^{\infty} (-1)^{\frac{m+1}{2}} \times \frac{4J_0^{\frac{mM\pi}{2}} 1}{m\pi z_{m\omega_c}} \sin\left(m\omega_c t - \frac{\pi}{2} - \theta_{m\omega_c}\right) + \sum_{m=1,3,5\ldots}^{\infty} \sum_{n=\pm 2,\pm 4,\ldots}^{\pm\infty} \frac{4J_n^{\frac{mM\pi}{2}}}{m\pi} \frac{1}{z_{m\omega_c + n\omega_m}} \times \sin\left(\frac{m\pi}{2}\right) \cos[(m\omega_c t + n\omega_m t) - m\pi - \theta_{m\omega_c} + n\omega_m] \right\}. \quad (6)$$

When this load current variation is reflected back to the clamping capacitor C_m, the corresponding clamping-capacitor-current variation $\Delta i_{\rm cm}$ is given by

$$\Delta i_{\rm cm} = \Delta i_{\rm load}({\rm SW}_1 - {\rm SW}_2). \quad (7)$$

Substituting from (1), (2) and (6) into (7), the result obtained for the clamping-capacitor-current variation is highly complicated allowing for little physical insight. However, when the clamping-capacitor-voltage is specifically concerned, only the dc component in the clamping-capacitor-current variation is of interest. This dc component in the clamping-capacitor-current variation $\Delta i_{\rm cm.dc}$ can finally be written as

$$\Delta i_{\rm cm.dc} = (V_{\rm cm.steady} - V_{\rm cm})G \quad (8)$$

where

$$G = \frac{1}{2} \sum_{m=1,3,5\ldots}^{\infty} \left\{ \left[(-1)^{\frac{m+1}{2}} \frac{4J_0^{\frac{mM\pi}{2}}}{m\pi} \right]^2 \frac{1}{z_{m\omega_c}} \cos(\theta_{m\omega_c}) \right\} + \frac{1}{2} \sum_{m=1,3,5\ldots}^{\infty} \sum_{n=\pm 2,\pm 4,\ldots}^{\pm\infty} \left\{ \left[\frac{4J_n^{\frac{mM\pi}{2}}}{m\pi} \sin\left(\frac{m\pi}{2}\right) \right]^2 \times \frac{1}{z_{m\omega_c + n\omega_m}} \cos(\theta_{m\omega_c} + n\omega_m) \right\}. \quad (9)$$

As the dc component in the clamping-capacitor-current at steady state is zero, $\Delta i_{\rm cm.dc}$ can be related to the clamping-capacitor-voltage $V_{\rm cm}$ by

$$(V_{\rm cm.steady} - V_{\rm cm})G = c_m \frac{dV_{\rm cm}}{dt}. \quad (10)$$

Then the clamping-capacitor-voltage transient can be given in the end by (11)

$$V_{\rm cm} = V_{\rm cm.steady} + [V_{\rm cm}(0) - V_{\rm cm.steady}] e^{-\frac{1}{\frac{C_m}{G}} t} \quad (11)$$

where

- $V_{\rm cm}(0)$ initial value of the clamping-capacitor-voltage during the transient;
- C_m capacitance of the clamping capacitor;
- C_m/G time constant of the transient which increases with the capacitance of the clamping capacitor, the load impedance amplitude, the load impedance angle and decreases with the modulation index.

During inverter starting, for example, the initial value of the clamping-capacitor-voltage $V_{\rm cm}(0)$ is zero.

From (8), (9), and (11), as constant G is always positive except for the case when the load is pure reactive, the dc component in the clamping-capacitor-current variation resulting from the clamping-capacitor-voltage deviation always counteracts such deviation, until the dc component in the clamping-capacitor-current variation becomes zero and the clamping-capacitor-voltage returns to its steady state value. It is in this sense, the clamping-capacitor-voltage is deemed self-balancing.

When the load is pure reactive, however, the cosine parts in (9) are zero and no dc component in the clamping-capacitor-current variation will be generated no matter how much is the clamping-capacitor-voltage deviation. The clamping-capacitor-voltage is then not self-balancing.

D. Steady State Clamping-Capacitor-Voltage

From the spontaneous clamping-capacitor-current control loop shown in Fig. 3, the clamping-capacitor-current is decided by the clamping-capacitor-voltage, the switching functions as well as the load impedance. With a given load, as the dc component in the clamping-capacitor-current must be zero at steady state, the steady state clamping-capacitor-voltage is solely decided by the switching functions. Ideally, under sub-harmonic PWM modulation, the steady state clamping-capacitor-voltage

is equal to its nominal value, i.e., $V_{\mathrm{cm.steady}} = V_{\mathrm{dc}}/2$. This result can be verified by following a similar calculation procedure as in SectionII-C and is not detailed.

Depending on asymmetric operation conditions which may arise in the system, such as mismatches in gating delays, device properties etc., however, the actual steady state clamping-capacitor-voltage under sub-harmonic PWM modulation may differ slightly from the nominal value $V_{\mathrm{dc}}/2$. When these asymmetries are insignificant, difference of the steady state clamping-capacitor-voltage from the nominal value will be negligible.

III. Self-Balancing of the Clamping-Capacitor-Voltages in the Multilevel Capacitor-Clamping-Inverter under Sub-Harmonic PWM Modulation

A. Mechanism of the Coupled Spontaneous Clamping-Capacitor-Current Control Loops

Fig. 4 shows a half-bridge $(n+1)$-level capacitor-clamping-inverter. When the inverter is modulated by sub-harmonic PWM technique with the carrier for each switching cell phase shifted by $2\pi/n$ [13], a spontaneous clamping-capacitor-current control loop can be identifPed for each clamping capacitor. However, the current control loop for any individual clamping capacitor is coupled with the remaining current control loops of the remaining clamping capacitors in the system by the load current, as illustrated in Fig. 5. As a result, deviation in any individual clamping-capacitor-voltage will contribute to the load voltage variation and in-turn the load current variation, affecting not only that individual clamping-capacitor-voltage but also the remaining clamPping-capacitor-voltages in the system.

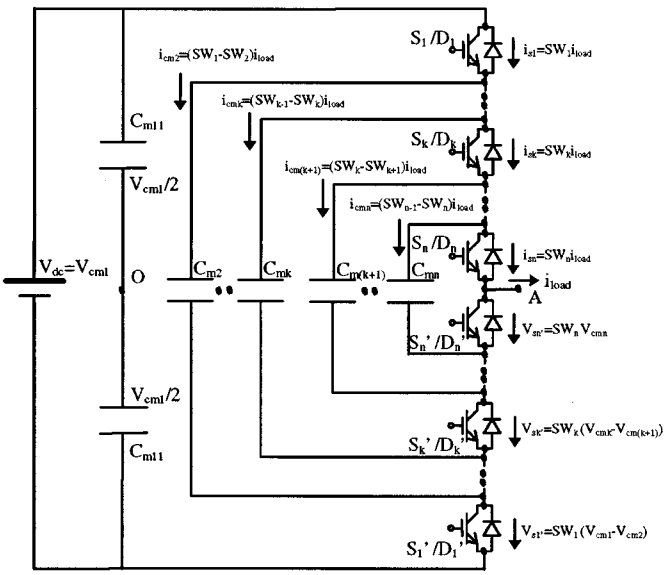

Fig. 4. Configuration of a half-bridge $(n+1)$-level capacitor-clamping-inverter.

B. Verification of the Coupled Spontaneous Clamping-Capacitor-Current Control Loops

For any initial state of the clamping-capacitor-voltages, the load voltage of the half-bridge inverter is given by

$$V_{\mathrm{AO}} = \mathrm{SW}_1(V_{\mathrm{cm1}} - V_{\mathrm{cm2}}) + \cdots + \mathrm{SW}_k\left(V_{\mathrm{cm}\,k} - V_{\mathrm{cm}\,(k+1)}\right) + \cdots \mathrm{SW}_n V_{\mathrm{cm}\,n} - \frac{V_{\mathrm{cm1}}}{2} \tag{12}$$

which is further expressed in

$$\begin{aligned} V_{\mathrm{AO}} = {} & (\mathrm{SW}_1 + \cdots + \mathrm{SW}_k + \cdots + \mathrm{SW}_n)\frac{V_{\mathrm{cm1}}}{n} - \frac{V_{\mathrm{cm1}}}{2} \\ & + (\mathrm{SW}_1 - \mathrm{SW}_2)\left(\frac{n-1}{n}V_{\mathrm{cm1}} - V_{\mathrm{cm2.steady}}\right) \\ & + \cdots + (\mathrm{SW}_{k-1} - \mathrm{SW}_k) \\ & \times \left(\frac{n-(k-1)}{n}V_{\mathrm{cm1}} - V_{\mathrm{cm}\,k.\mathrm{steady}}\right) \\ & + \cdots + (\mathrm{SW}_{n-1} - \mathrm{SW}_n)\left(\frac{1}{n}V_{\mathrm{cm1}} - V_{\mathrm{cm}\,n.\mathrm{steady}}\right) \\ & + (\mathrm{SW}_1 - \mathrm{SW}_2)(V_{\mathrm{cm2.steady}} - V_{\mathrm{cm2}}) \\ & + \cdots + (\mathrm{SW}_{k-1} - \mathrm{SW}_k)(V_{\mathrm{cm}\,k.\mathrm{steady}} - V_{\mathrm{cm}\,k}) \\ & + \cdots + (\mathrm{SW}_{n-1} - \mathrm{SW}_n)(V_{\mathrm{cm}\,n.\mathrm{steady}} - V_{\mathrm{cm}\,n}) \end{aligned} \tag{13}$$

where $((n-(k-1))/n)V_{\mathrm{cm1}}$ is the nominal value of the k-th clamping-capacitor-voltage and $V_{\mathrm{cm}\,k.\mathrm{steady}}$ is the steady state value of the k-th clamping-capacitor-voltage. The load voltage

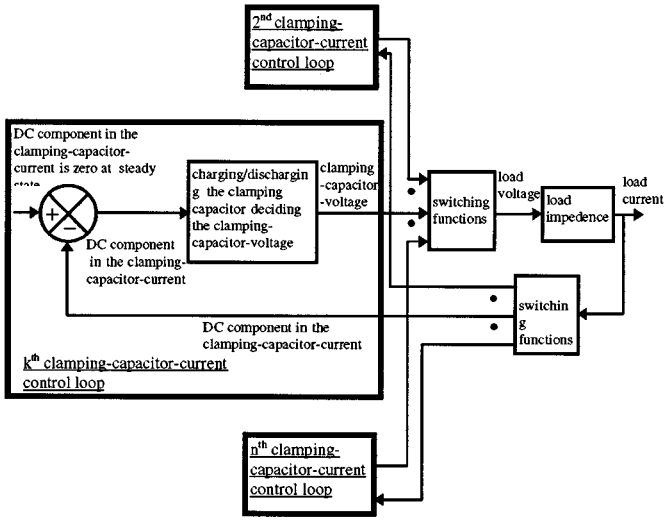

Fig. 5. Coupled spontaneous clamping-capacitor-current control loops in the half-bridge $(n+1)$-level capacitor-clamping-inverter.

variation in response to the deviations of the clamping-capacitor-voltages from their corresponding steady state values is given by the third line in (13) and is noted in

$$\begin{aligned} \Delta V_{\mathrm{AO}} = {} & (\mathrm{SW}_1 - \mathrm{SW}_2)(V_{\mathrm{cm2.steady}} - V_{\mathrm{cm2}}) \\ & + \cdots + (\mathrm{SW}_{k-1} - \mathrm{SW}_k)(V_{\mathrm{cm}\,k.\mathrm{steady}} - V_{\mathrm{cm}\,k}) \\ & + \cdots + (\mathrm{SW}_{n-1} - \mathrm{SW}_n)(V_{\mathrm{cm}\,n.\mathrm{steady}} - V_{\mathrm{cm}\,n}). \end{aligned} \tag{14}$$

Note that $\mathrm{SW}_{k-1} - \mathrm{SW}_k$ contains components of odd multiples of the switching frequency. (14) can be rewritten as

$$\begin{aligned} \Delta V_{\mathrm{AO}} = {} & \sum_{i=1,3,5\ldots}^{\infty} \overrightarrow{\mathrm{SW}}_{12.i\,\mathrm{fc}}\,(V_{\mathrm{cm2.steady}} - V_{\mathrm{cm2}}) \\ & + \cdots + \overrightarrow{\mathrm{SW}}_{(k-1)k.i\,\mathrm{fc}}\,(V_{\mathrm{cm}\,k.\mathrm{steady}} - V_{\mathrm{cm}\,k}) \\ & + \cdots + \overrightarrow{\mathrm{SW}}_{(n-1)n.i\,\mathrm{fc}}\,(V_{\mathrm{cm}\,n.\mathrm{steady}} - V_{\mathrm{cm}\,n}) \end{aligned} \tag{15}$$

where $\vec{\mathrm{SW}}_{(k-1)k.i\,\mathrm{fc}}$ represents the i-th switching frequency component in $\mathrm{SW}_{(k-1)} - \mathrm{SW}_k$.

For simplicity, the fundamental switching frequency component ($i = 1$) is taken into account first. The corresponding load current variation resulting from the fundamental switching frequency component in the load voltage variation $\Delta i_{\mathrm{load.fc}}$ can be expressed in

$$\begin{aligned}\Delta i_{\mathrm{load.fc}} = {} & \frac{\vec{\mathrm{SW}}_{12.\mathrm{fc}}}{\vec{Z}_{\mathrm{load.fc}}}(V_{\mathrm{cm2.steady}} - V_{\mathrm{cm2}}) \\ & + \cdots + \frac{\vec{\mathrm{SW}}_{(k-1)k.\mathrm{fc}}}{\vec{Z}_{\mathrm{load.fc}}}(V_{\mathrm{cm}\,k.\mathrm{steady}} - V_{\mathrm{cm}\,k}) \\ & + \cdots + \frac{\vec{\mathrm{SW}}_{(n-1)n.\mathrm{fc}}}{\vec{Z}_{\mathrm{load.fc}}}(V_{\mathrm{cm}\,n.\mathrm{steady}} - V_{\mathrm{cm}\,n}) \quad (16)\end{aligned}$$

where $\vec{Z}_{\mathrm{load.fc}}$ is the load impedance at the fundamental switching frequency.

The corresponding variation of the k-th clamping-capacitor-current resulting from the fundamental switching frequency component in the load voltage variation can be given by

$$\Delta i_{\mathrm{cm}\,k.\mathrm{fc}} = \left(\mathrm{SW}_{(k-1)} - \mathrm{SW}_k\right)\Delta i_{\mathrm{load.fc}}. \quad (17)$$

According to the principle of perpendicularity, multiplication of two sinusoidal functions of different frequencies can be averaged to zero, then (17) can be simplified to

$$\begin{aligned}\Delta i_{\mathrm{cm}\,k.\mathrm{fc}} = {} & \vec{\mathrm{SW}}_{(k-1)k.\mathrm{fc}}\,\Delta i_{\mathrm{load.fc}} \\ = {} & \vec{\mathrm{SW}}_{(k-1)k.\mathrm{fc}}\left[\frac{\vec{\mathrm{SW}}_{12.\mathrm{fc}}}{\vec{Z}_{\mathrm{load.fc}}}(V_{\mathrm{cm2.steady}} - V_{\mathrm{cm2}})\right. \\ & + \cdots + \frac{\vec{\mathrm{SW}}_{(k-1)k.\mathrm{fc}}}{\vec{Z}_{\mathrm{load.fc}}}(V_{\mathrm{cm}\,k.\mathrm{steady}} - V_{\mathrm{cm}\,k}) \\ & \left. + \cdots + \frac{\vec{\mathrm{SW}}_{(n-1)n.\mathrm{fc}}}{\vec{Z}_{\mathrm{load.fc}}}(V_{\mathrm{cm}\,n.\mathrm{steady}} - V_{\mathrm{cm}\,n})\right]. \quad (18)\end{aligned}$$

The variation of the k-th clamping capacitor current resulted from all harmonic components in the load voltage variation is then given in

$$\Delta i_{\mathrm{cm}\,k} = \sum_{i=1,3,5\ldots}^{\infty} \Delta i_{\mathrm{cm}\,k.i\,\mathrm{fc}} \quad (19)$$

where $\Delta i_{\mathrm{cm}\,k.i\,\mathrm{fc}}$ represents the variation of the k-th clamping capacitor current resulted from the i-th switching frequency component in the load voltage variation and can be detailed by

$$\begin{aligned}\Delta i_{\mathrm{cm}\,k.i\,\mathrm{fc}} = {} & \vec{\mathrm{SW}}_{(k-1)k.i\,\mathrm{fc}}\,\Delta i_{\mathrm{load.}i\,\mathrm{fc}} \\ = {} & \vec{\mathrm{SW}}_{(k-1)k.i\,\mathrm{fc}} \\ & \times \left[\frac{\vec{\mathrm{SW}}_{12.i\,\mathrm{fc}}}{\vec{\mathrm{Z}}_{\mathrm{load.}i\,\mathrm{fc}}}(V_{\mathrm{cm2.steady}} - V_{\mathrm{cm2}})\right. \\ & + \cdots + \frac{\vec{\mathrm{SW}}_{(k-1)k.i\,\mathrm{fc}}}{\vec{\mathrm{Z}}_{\mathrm{load.}i\,\mathrm{fc}}}(V_{\mathrm{cm}\,k.\mathrm{steady}} - V_{\mathrm{cm}\,k}) \\ & \left. + \cdots + \frac{\vec{\mathrm{SW}}_{(n-1)n.i\,\mathrm{fc}}}{\vec{\mathrm{Z}}_{\mathrm{load.}i\,\mathrm{fc}}}(V_{\mathrm{cm}\,n.\mathrm{steady}} - V_{\mathrm{cm}\,n})\right] \quad (20)\end{aligned}$$

where $\vec{\mathrm{Z}}_{\mathrm{load.}i\,\mathrm{fc}}$ is the load impedance at the i-th switching frequency.

Again, the variation of the k-th clamping-capacitor-current can be related to the k-th clamping capacitor voltage by

$$\Delta i_{\mathrm{cm}\,k} = C_{mk}\frac{dV_{\mathrm{cm}\,k}}{dt} = -C_{mk}\frac{d(V_{\mathrm{cm}\,k.\mathrm{steady}} - V_{\mathrm{cm}\,k})}{dt}. \quad (21)$$

Combining (18)–(21), the transients of the clamping-capacitor-voltages following the deviations of the clamping-capacitor-voltages from their corresponding steady state values can be described by (22), shown at the bottom of the page, where $\Delta V_{\mathrm{cm}\,k} = V_{\mathrm{cm}\,k.\mathrm{steady}} - V_{\mathrm{cm}\,k}$ represents the variation of the k-th clamping capacitor voltage from its steady state value.

This homogeneous state space equation can be solved by the state transfer matrix approach [15]. For the three-level case ($n = 2$), (22) is equivalent to (11). For the four-level case ($n = 3$), provided that $C_{m2} = C_{m3} = C$, the transients of the clamping-capacitor-voltages can be obtained in

$$\begin{aligned}\begin{bmatrix}\Delta V_{\mathrm{cm2}} \\ \Delta V_{\mathrm{cm3}}\end{bmatrix} = {} & \begin{bmatrix} L_1 e^{\frac{-1}{C}\frac{t}{G_1}} + L_2 e^{\frac{-1}{C}\frac{t}{G_2}} & L_3 e^{\frac{-1}{C}\frac{t}{G_3}} + L_4 e^{\frac{-1}{C}\frac{t}{G_4}} \\ L_5 e^{\frac{-1}{C}\frac{t}{G_5}} + L_6 e^{\frac{-1}{C}\frac{t}{G_6}} & L_7 e^{\frac{-1}{C}\frac{t}{G_7}} + L_8 e^{\frac{-1}{C}\frac{t}{G_8}} \end{bmatrix} \\ & \times \begin{bmatrix}\Delta V_{\mathrm{cm2}}(0) \\ \Delta V_{\mathrm{cm3}}(0)\end{bmatrix} \quad (23)\end{aligned}$$

where you get (24) and (25), shown at the bottom of the next page.

$$\begin{bmatrix}\Delta\dot{V}_{\mathrm{cm2}} \\ \bullet \\ \Delta\dot{V}_{\mathrm{cm}\,k} \\ \bullet \\ \Delta\dot{V}_{\mathrm{cm}\,n}\end{bmatrix} = \sum_{i=1,3,5\ldots}^{\infty} \begin{bmatrix} \frac{-\vec{\mathrm{SW}}_{12.i\,\mathrm{fc}}\vec{\mathrm{SW}}_{12.i\,\mathrm{fc}}}{C_{m2}\vec{\mathrm{Z}}_{\mathrm{load.}i\,\mathrm{fc}}} & \bullet & \frac{-\vec{\mathrm{SW}}_{12.i\,\mathrm{fc}}\vec{\mathrm{SW}}_{(k-1)k.i\,\mathrm{fc}}}{C_{m2}\vec{\mathrm{Z}}_{\mathrm{load.}i\,\mathrm{fc}}} & \bullet & \frac{-\vec{\mathrm{SW}}_{12.i\,\mathrm{fc}}\vec{\mathrm{SW}}_{(n-1)n.i\,\mathrm{fc}}}{C_{m2}\vec{\mathrm{Z}}_{\mathrm{load.}i\,\mathrm{fc}}} \\ \bullet & & \bullet & & \bullet \\ \frac{-\vec{\mathrm{SW}}_{(k-1)k.i\,\mathrm{fc}}\vec{\mathrm{SW}}_{12.i\,\mathrm{fc}}}{C_{mk}\vec{\mathrm{Z}}_{\mathrm{load.}i\,\mathrm{fc}}} & \bullet & \frac{-\vec{\mathrm{SW}}_{(k-1)k.i\,\mathrm{fc}}\vec{\mathrm{SW}}_{(k-1)k.i\,\mathrm{fc}}}{C_{mk}\vec{\mathrm{Z}}_{\mathrm{load.}i\,\mathrm{fc}}} & \bullet & \frac{-\vec{\mathrm{SW}}_{(k-1)k.i\,\mathrm{fc}}\vec{\mathrm{SW}}_{(n-1)n.i\,\mathrm{fc}}}{C_{mk}\vec{\mathrm{Z}}_{\mathrm{load.}i\,\mathrm{fc}}} \\ \bullet & & \bullet & & \bullet \\ \frac{-\vec{\mathrm{SW}}_{(n-1)n.i\,\mathrm{fc}}\vec{\mathrm{SW}}_{12.i\,\mathrm{fc}}}{C_{mn}\vec{\mathrm{Z}}_{\mathrm{load.}i\,\mathrm{fc}}} & \bullet & \frac{-\vec{\mathrm{SW}}_{(n-1)n.i\,\mathrm{fc}}\vec{\mathrm{SW}}_{(k-1)k.i\,\mathrm{fc}}}{C_{mn}\vec{\mathrm{Z}}_{\mathrm{load.}i\,\mathrm{fc}}} & \bullet & \frac{-\vec{\mathrm{SW}}_{(n-1)n.i\,\mathrm{fc}}\vec{\mathrm{SW}}_{(n-1)n.i\,\mathrm{fc}}}{C_{mn}\vec{\mathrm{Z}}_{\mathrm{load.}i\,\mathrm{fc}}} \end{bmatrix} \times \begin{bmatrix}\Delta V_{\mathrm{cm2}} \\ \bullet \\ \Delta V_{\mathrm{cm}\,k} \\ \bullet \\ \Delta V_{\mathrm{cm}\,n}\end{bmatrix} \quad (22)$$

Note that coefficients L_1–L_8 are functions of SW_{12} and SW_{23}. Since they do not affect the convergence property of the equation, they are not detailed. Considering scalar multiplication of two vectors, (26)–(28) are true

$$\vec{\mathrm{SW}}_{12.i\,\mathrm{fc}}\,\frac{\vec{\mathrm{SW}}_{12.i\,\mathrm{fc}}}{\vec{\mathrm{Z}}_{\mathrm{load}.i\,\mathrm{fc}}} = \vec{\mathrm{SW}}_{23.i\,\mathrm{fc}}\,\frac{\vec{\mathrm{SW}}_{23.i\,\mathrm{fc}}}{\vec{\mathrm{Z}}_{\mathrm{load}.i\,\mathrm{fc}}} = \frac{|\,\vec{\mathrm{SW}}_{12.i\,\mathrm{fc}}\,|^2}{|\,\vec{\mathrm{Z}}_{\mathrm{load}.i\,\mathrm{fc}}\,|}\cos(\angle\,\vec{\mathrm{Z}}_{\mathrm{load}.i\,\mathrm{fc}}) \quad (26)$$

$$\vec{\mathrm{SW}}_{23.i\,\mathrm{fc}}\,\frac{\vec{\mathrm{SW}}_{12.i\,\mathrm{fc}}}{\vec{\mathrm{Z}}_{\mathrm{load}.i\,\mathrm{fc}}} = \frac{|\,\vec{\mathrm{SW}}_{12.i\,\mathrm{fc}}\,|^2}{|\,\vec{\mathrm{Z}}_{\mathrm{load}.i\,\mathrm{fc}}\,|} \times \cos(\angle\,\vec{\mathrm{SW}}_{23.i\,\mathrm{fc}} - \angle\,\vec{\mathrm{SW}}_{12.i\,\mathrm{fc}} + \angle\,\vec{\mathrm{Z}}_{\mathrm{load}.i\,\mathrm{fc}}) \quad (27)$$

$$\vec{\mathrm{SW}}_{12.i\,\mathrm{fc}}\,\frac{\vec{\mathrm{SW}}_{23.i\,\mathrm{fc}}}{\vec{\mathrm{Z}}_{\mathrm{load}.i\,\mathrm{fc}}} = \frac{|\,\vec{\mathrm{SW}}_{12.i\,\mathrm{fc}}\,|^2}{|\,\vec{\mathrm{Z}}_{\mathrm{load}.i\,\mathrm{fc}}\,|} \times \cos(\angle\,\vec{\mathrm{SW}}_{23.i\,\mathrm{fc}} - \angle\,\vec{\mathrm{SW}}_{12.i\,\mathrm{fc}} - \angle\,\vec{\mathrm{Z}}_{\mathrm{load}.i\,\mathrm{fc}}). \quad (28)$$

As a result, (24) and (25) can be simplified to (29) and (30), respectively, shown at the bottom of the page.

Examining the expressions for the transients of clamping-capacitor-voltages given in (23), and the expressions for G_1–G_8 given in (29) and (30), when the load is pure reactive, the real parts of G_1–G_8 are always zero, the clamping-capacitor-voltages are not self-balancing. When the load is not pure reactive, however, the real parts of G_1–G_8 are always positive, the clamping-capacitor-voltages become self-balancing. The time constants of the transients are dependent on the capacitances of the clamping capacitors, the load impedance and the switching functions in the same relationships as the three-level case discussed in Section II.

Capacitor-clamping-inverter above four-level has limited practical interest and is not detailed.

C. Steady State Clamping-Capacitor-Voltages

Following a similar calculation procedure as in part B of this section, it can be verified that under sub-harmonic PWM modulation, the dc components of the clamping-capacitor-currents will be zero when the clamping-capacitor-voltages are equal to the nominal values. This implies that under sub-harmonic PWM modulation, the steady state clamping-capacitor-voltages are equal to the nominal values.

Again, when asymmetric operation conditions in the system are taken into account, slight differences between the steady state values and the nominal values may exist. When these asymmetries are insignificant, the differences will be negligible.

IV. Experimentation

A scaled half-bridge three-level capacitor-clamping-inverter prototype (without the auxiliary starting network) was estab-

$$G_1 = G_3 = G_5 = G_7 = \sum_{i=1,3,5\ldots}^{\infty} \frac{\left(\vec{\mathrm{SW}}_{12.i\mathrm{fc}}\,\frac{\vec{\mathrm{SW}}_{12.i\mathrm{fc}}}{\vec{\mathrm{Z}}_{\mathrm{load}.i\mathrm{fc}}} + \vec{\mathrm{SW}}_{23.i\mathrm{fc}}\,\frac{\vec{\mathrm{SW}}_{23.i\mathrm{fc}}}{\vec{\mathrm{Z}}_{\mathrm{load}.i\mathrm{fc}}}\right)}{2} + \frac{\sqrt{\left(\vec{\mathrm{SW}}_{12.i\mathrm{fc}}\,\frac{\vec{\mathrm{SW}}_{12.i\mathrm{fc}}}{\vec{\mathrm{Z}}_{\mathrm{load}.i\mathrm{fc}}} - \vec{\mathrm{SW}}_{23.i\mathrm{fc}}\,\frac{\vec{\mathrm{SW}}_{23.i\mathrm{fc}}}{\vec{\mathrm{Z}}_{\mathrm{load}.i\mathrm{fc}}}\right)^2 + 4\left(\vec{\mathrm{SW}}_{23.i\mathrm{fc}}\,\frac{\vec{\mathrm{SW}}_{12.i\mathrm{fc}}}{\vec{\mathrm{Z}}_{\mathrm{load}.i\mathrm{fc}}}\right)\left(\vec{\mathrm{SW}}_{12.i\mathrm{fc}}\,\frac{\vec{\mathrm{SW}}_{23.i\mathrm{fc}}}{\vec{\mathrm{Z}}_{\mathrm{load}.i\mathrm{fc}}}\right)}}{2} \quad (24)$$

$$G_2 = G_4 = G_6 = G_8 = \sum_{i=1,3,5\ldots}^{\infty} \frac{\left(\vec{\mathrm{SW}}_{12.i\mathrm{fc}}\,\frac{\vec{\mathrm{SW}}_{12.i\mathrm{fc}}}{\vec{\mathrm{Z}}_{\mathrm{load}.i\mathrm{fc}}} + \vec{\mathrm{SW}}_{23.i\mathrm{fc}}\,\frac{\vec{\mathrm{SW}}_{23.i\mathrm{fc}}}{\vec{\mathrm{Z}}_{\mathrm{load}.i\mathrm{fc}}}\right)}{2} - \frac{\sqrt{\left(\vec{\mathrm{SW}}_{12.i\mathrm{fc}}\,\frac{\vec{\mathrm{SW}}_{12.i\mathrm{fc}}}{\vec{\mathrm{Z}}_{\mathrm{load}.i\mathrm{fc}}} - \vec{\mathrm{SW}}_{23.i\mathrm{fc}}\,\frac{\vec{\mathrm{SW}}_{23.i\mathrm{fc}}}{\vec{\mathrm{Z}}_{\mathrm{load}.i\mathrm{fc}}}\right)^2 + 4\left(\vec{\mathrm{SW}}_{23.i\mathrm{fc}}\,\frac{\vec{\mathrm{SW}}_{12.i\mathrm{fc}}}{\vec{\mathrm{Z}}_{\mathrm{load}.i\mathrm{fc}}}\right)\left(\vec{\mathrm{SW}}_{12.i\mathrm{fc}}\,\frac{\vec{\mathrm{SW}}_{23.i\mathrm{fc}}}{\vec{\mathrm{Z}}_{\mathrm{load}.i\mathrm{fc}}}\right)}}{2} \quad (25)$$

$$G_1 = G_3 = G_5 = G_7 = \sum_{i=1,3,5\ldots}^{\infty}\left\{\frac{|\,\vec{\mathrm{SW}}_{12.i\,\mathrm{fc}}\,|^2}{|\,\vec{\mathrm{Z}}_{\mathrm{load}.i\,\mathrm{fc}}\,|}\left[\cos(\angle\,\vec{\mathrm{Z}}_{\mathrm{load}.i\,\mathrm{fc}}) + \sqrt{\cos^2(\angle\,\vec{\mathrm{SW}}_{23.i\,\mathrm{fc}} - \angle\,\vec{\mathrm{SW}}_{12.i\,\mathrm{fc}}) + \cos^2(\angle\,\vec{\mathrm{Z}}_{\mathrm{load}.i\,\mathrm{fc}}) - 1}\right]\right\} \quad (29)$$

$$G_2 = G_4 = G_6 = G_8 = \sum_{i=1,3,5\ldots}^{\infty}\left\{\frac{|\,\vec{\mathrm{SW}}_{12.i\,\mathrm{fc}}\,|^2}{|\,\vec{\mathrm{Z}}_{\mathrm{load}.i\,\mathrm{fc}}\,|}\left[\cos(\angle\,\vec{\mathrm{Z}}_{\mathrm{load}.i\,\mathrm{fc}}) - \sqrt{\cos^2(\angle\,\vec{\mathrm{SW}}_{23.i\,\mathrm{fc}} - \angle\,\vec{\mathrm{SW}}_{12.i\,\mathrm{fc}}) + \cos^2(\angle\,\vec{\mathrm{Z}}_{\mathrm{load}.i\,\mathrm{fc}}) - 1}\right]\right\} \quad (30)$$

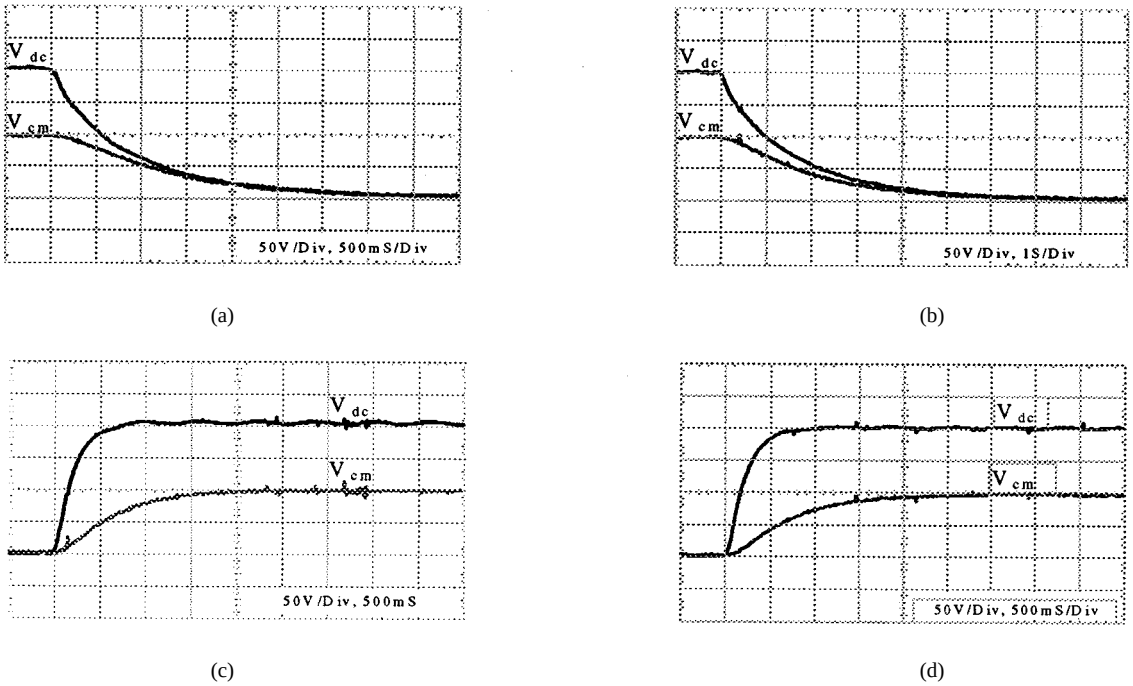

Fig. 6. Test results of the clamping-capacitor-voltage self-balancing in the half-bridge capacitor-clamping-inverter, with different load resistances when the dc supply is switched off and on: (a) dc supply switched off, load resistance $R_o = 3\ \Omega$, (b) dc supply switched off, load resistance $R_o = 7.5\ \Omega$, (c) dc supply switched on, load resistance $R_o = 3\ \Omega$, and (d) dc supply switched on, load resistance $R_o = 7.5\ \Omega$.

lished in the laboratory. The sub-harmonic PWM modulation discussed in Fig. 2 was employed. Parameters and specifications of the prototype are: dc input voltage $V_{\rm dc} = 200$ V, clamping capacitance $C_m = 1650$ uF, switching frequency $f_c = 6.5$ kHz, modulation index $M = 0.62$, output filter $L_f = 1.45$ mH and $C_f = 12$ uF. Test results with different load resistances when the dc supply is switched-off and switched-on are shown in Fig. 6(a)–(d). From the results, on the one hand, the clamping-capacitor-voltage is self-balancing and the steady state value is almost equal to the nominal value (100 V). On the other hand, the time constant of the transient increases with the load resistance. The analyses in Section II are verified.

V. Conclusion

From the analyses and test results presented in the paper, the following conclusions are drawn.

1) Due to the spontaneous clamping-capacitor-current control loop, the clamping-capacitor-voltage in the three-level capacitor-claming-inverter is self-balancing under sub-harmonic PWM modulation when the load is not pure-reactive. The time constant of the clamping-capacitor-voltage transient increases with the capacitance of the clamping capacitor, the load impedance amplitude, the load impedance angle and decreases with the modulation index. The steady state clamping-capacitor-voltage is equal to the nominal value under sub-harmonic PWM modulation. When asymmetries in the system are taken into account, slight difference between the steady state value and the nominal value may exist. When the asymmetries are insignificant, the difference will be negligible.
2) For multilevel capacitor-clamping-inverter $(M > 3)$ under sub-harmonic PWM modulation, the spontaneous current control loop of an individual clamping capacitor is coupled with the remaining control loops for the remaining clamping capacitors by the load current. Similarly, the clamping-capacitor-voltages are self-balancing when the load is not pure-reactive, with the time constants of the transients dependent on the capacitances of the clamping capacitors, the load impedance and the switching functions, in the same relatonships as the three-level case.
3) Due to self-balancing of the clamping-capacitor-voltages, multilevel capacitor-clamping-inverter under sub-harmonic PWM modulation may work without active control of the clamping-capacitor-voltages. This possibility enables significant reduction of the control complexity. To deal with operation conditions with weak self-balancing (light load, reactive load and low modulation index etc.), a pesudo load may be needed for enhancing the self-balancing.

References

[1] J. S. Lai and F. Z. Peng, "Multilevel converters—A new breed of power converters," in *Proc. IEEE Ind. Applicat. Soc. Annu. Meeting*, 1995, pp. 2348–2356.
[2] C. Hochgraf, R. Lasseter, D. Divan, and T. Lipo, "Comparison of multilevel inverters for static var compensation," in *Proc. IEEE Ind. Applicat. Soc. Annu. Meeting*, 1994, pp. 921–928.
[3] F. Z. Peng, J. S. Lai, J. Mckeever, and J. VanCoevering, "A multilevel voltage source converter system with balanced dc voltages," in *Proc. IEEE Power Electron. Specialists Conf.*, 1995, pp. 1144–1150.
[4] G. Sinha and T. Lipo, "A four level inverter based drive with a passive front end," in *Proc. IEEE Power Electron. Spec. Conf.*, 1997, pp. 590–596.

[5] X. Yuan and I. Barbi, "Fundamentals of a new diode clamping multilevel inverter," *IEEE Trans. Power Electron.*, vol. 15, pp. 711–718, July 2000.
[6] P. W. Hammond, "A new approach to enhance power quality for medium voltage AC drives," *IEEE Trans. Ind. Applicat.*, vol. 33, no. 1, pp. 202–208, Jan./Feb. 1997.
[7] J. D. Ainsworth, M. Davies, P. J. Fitz, K. E. Owen, and D. R. Trainer, "Static var compensator (STATCOM) based on single-phase chain circuit converters," in *Proc. Inst. Elect. Eng.—Gener. Transm. Distrib.*, vol. 145, July 1998, pp. 381–386.
[8] M. D. Manjrekar, P. Steimer, and T. A. Lipo, "Hybrid multilevel power conversion system: A competitive solution for high power applications," in *Proc. IEEE Ind. Applicat. Soc. Annu. Meeting*, 1999, pp. 1520–1527.
[9] M. Steiner, R. Deplazes, and H. Stemmler, "A new transformerless topology for AC-fed traction vehicles using multi-star induction motors," in *Proc. European Conf. Power Electron. Applicat.*, 1999.
[10] E. Cengelci, P. Enjeti, C. Singh, F. Blaabjerg, and J. K. Pederson, "New medium voltage PWM inverter topologies for adjustable seed AC motor drive systems," in *Proc. IEEE Appl. Power Electron. Conf.*, 1998, pp. 565–571.
[11] Y. Shakweh and E. A. Lewis, "Assessment of medium voltage PWM VSI topologies for multi-megawatt variable speed drive applications," in *Proc. IEEE Power Electron. Spec. Conf.*, 1999, pp. 965–971.
[12] J. Courault, O. Lapierre, and J. L. Pouliquen, "Industrial interests of multilevel converters," in *Proc. Euro. Conf. Power Electron. Applicat.*, 1999.
[13] P. Carrère, T. Meynard, and J. P. Lavieville, "4000 V-300 A eight-level IGBT inverter leg," in *Proc. Euro. Conf. Power Electron. Applicat.*, 1995, pp. 1106–1111.
[14] A. Schonung and H. Stemmler, "Static frequency changers with sub-harmonic control in conjection with reversable variable speed AC drives," *Brown Boveri Rev.*, vol. 51, no. 8/9, pp. 555–577, Sept. 1964.
[15] S. Cai, *Automatic Control Theory*, Beijing, China: Machinery Industry, 1980.

Xiaoming Yuan (S'97–M'99) received the B.Eng. degree from Shandong University, China, in 1986, the M.Eng. degree from Zhejiang University, Hangzhou, China, in 1993, and the Ph.D. degree from the Federal University of Santa Catarina, Brazil, in 1998, all in electrical engineering.

He was an Electrical Engineer with Qilu Petrochemical Corporation, China, from 1986 to 1990. He is currently a Postdoctoral Researcher with the Power Electronics and Electrometrology Laboratory, Swiss Federal Institute of Technology, Zurich, Switzerland.

Dr. Yuan received the first prize paper award from the Industrial Power Converter Committee of the IEEE Industry Applications Society in 1999.

Herbert Stemmler received the Dipl.-Ing. degree in automation from the Techniche Hochschule, Darmsdadt, Germany, in 1961, and the Ph.D. degree in power electronics from the Technische Hochschule, Aachen, Germany, in 1971.

He worked with Brown Bovery and ASEA-Brown Bovery, Baden, Switzerland, from 1961 to 1991, in the field of power electronics. From 1971 to 1991, he was head of the department for development, engineering, test, and commissioning of large power electronics systems. In 1987, he was appointed Vice President of this department. During these years, he worked with converter and inverter locomotives, 50-16 2/3 Hz inverters, all kinds of large ac drives, reactive power compensators, HVDC transmissions, low-power electronics, standardized, and tailor-made electronic control units. Since 1991, he has been Professor of Power Electronics at the Swiss Federal Institute of Technology, Zurich, Switzerland, and Head of the Power Electronics and Electrometrology Laboratory. At the time there have been 15 doctoral projects completed and seven projects ongoing in traction, motor drives, flexible-ac-transmission-systems (FACTS), solar energy systems, uninterruptable power supplies, matrix converters, and fuel cell vehicles.

Ivo Barbi (M'78–SM'90) was born in Gaspar, Santa Catarina, Brazil in 1949. He received the B.S. and M.S. degrees in electrical engineering from the Federal University of Santa Catarina, Florianopolis, in 1973 and 1976, respectively, and the Dr. Ing. degree from the Institut National Polytechnique de Toulouse, France, in 1979.

He founded the Brazilian Power Electronics Society, the Power Electronics Institute, Federal University of Santa Catarina, and created the Brazilian Power Electronics Conference. Currently, he is Professor of the Power Electronics Institute, Federal University of Santa Catarina.

Dr. Barbi has been and Associate Editor in the Power Converters Area, IEEE TRANSACTIONS ON INDUSTRIAL ELECTRONICS, since January 1992.